Energy transfer in Ce, Nd, and Yb co-doped YAG phosphors

Lulu Wang (王璐璐)[1,2], Changtai Xia (夏长泰)[1*], Peng Xu (许 鹏)[1,2], Juqing Di (狄聚青)[1,2], Qinglin Sai (赛青林)[1,2], and Fei Mou (牟 菲)[1,2]

[1] *Key Laboratory of Materials for High Power Laser, Shanghai Institute of Optics and Fine Mechanics, Chinese Academy of Sciences, Shanghai 201800, China*

[2] *University of Chinese Academy of Sciences, Beijing 100049, China*

[*] *Corresponding author: Xia_CT@siom.ac.cn*

Received January 28, 2013; accepted March 29, 2013; posted online May 30, 2013

YAG-Ce, Nd, and Yb phosphors with a triple-doped system are prepared by conventional solid-state reaction method. The fluorescence emission and excitation spectra are measured and analyzed. The influences of Yb^{3+} doping concentration on the emission of Yb^{3+} and Nd^{3+} in YAG-Ce, Nd, and Yb are studied. The fluorescence decay spectra, lifetime, and energy transfer efficiency of Ce^{3+} in different host materials of YAG-Ce and Yb, and YAG-Ce, Nd, and Yb are also compared. Furthermore, the trends of fluorescence decay spectra and the lifetimes of Nd^{3+} and Yb^{3+} in YAG-Ce, Nd, and Yb with the increase of Yb^{3+}concentration are discussed. Results indicate that YAG-Ce, Nd, and Yb are good candidates for downconverting phosphor, with energy transfer efficiency reaching as high as 82.8%.

OCIS codes: 160.4670, 160.4760, 160.4890, 160.5690.

doi: 10.3788/COL201311.061604.

Trivalent rare earth (RE^{3+}) ion-doped luminescent materials receive constant attention due to their extensive applications, especially in phosphors for white light-emitting diodes (LEDs), displays, and optical amplifiers in telecommunication. They are also used in photovoltaic cells by direct conversion of solar energy to meet the long-term energy demand. The strongest emission of the solar spectrum is about 350 to 550 nm. Trupke *et al.*[1] demonstrated that the optimum underlying solar cell band gap was close to 1.1 eV (∼1 100 nm). Although crystal silicon (c-Si) solar cells dominate the market[2], their low efficiency of about 29%[3] restricts further application, which is mainly caused by the mismatch between the incident solar spectrum and the spectral response of solar cells[1,4]. Downconverting phosphor by converting one photon of high energy into two photons of lower energy is a promising technique for improving solar cell efficiency[5,6].

Based on energy match with Si solar cell, $Yb^{3+}$with intense emission peak at 1 029 nm and Nd^{3+} with emission peak at 1 064 nm are good candidates. RE ion pairs, such as Tb^{3+}, Tm^{3+}, Pr^{3+}-Yb^{3+}, and Eu^{3+}-Nd^{3+}, reportedly enhance the cells' efficiency[7−10]. However, due to the partly forbidden f→f transition of the above sensitizer ions, their luminescence intensities are rather weak and their peak bandwidths are narrow. Unlike other RE ions, Ce^{3+} with allowed 5d→4f transition could be a good sensitizing ion. More importantly, the emission energy of 5d→4f matches about twice the energy of $^2F_{5/2} \rightarrow {}^2F_{7/2}$ transition of Yb^{3+}. Lin *et al.*[11] reported on Yb-doped $Ce_{0.03}Yb_{3x}Y_{(2.97-3x)}Al_5O_{12}$ transparent ceramics. The energy transfer was demonstrated by excitation, emission, and time-resolved luminescence. Ce and Yb co-doped ceramics may have practical applications in enhancing the conversion of crystalline Si solar cells due to the 175.4% quantum yield. Such phenomenon has also been reported in single crystals[12] and phosphors[13]. The energy transfer from $Ce^{3+}$to Nd^{3+} in the YAG matrix was experimentally studied by Meng *et al.*[14,15]. Under 476-nm excitation, YAG-Ce and Nd produce strong NIR emission with high quantum yield. Consequently, energy transfer from Ce^{3+} to Yb^{3+} and from Ce^{3+} to Nd^{3+} occurs. This finding prompts us to study the possible energy transfer with a process of Ce^{3+}, namely, 5d→Nd^{3+}: $^2G_{9/2}$ →Yb^{3+}: $^2F_{5/2}$, which may develop better NIR fluorescence phosphor in a triple-doped system and become a promising candidate for improving solar cell efficiency.

On this premise, Ce, Nd, and Yb co-doping in YAG phosphors are investigated in this letter. The energy transfer is evaluated by the emission and excitation spectra, fluorescence decay spectra, decay lifetime, and energy transfer efficiency. The dependence of Yb^{3+} concentration on the emission of Yb^{3+} and Nd^{3+} and the decay lifetime of Ce^{3+}, Nd^{3+}, and Yb^{3+} are also reported.

YAG-Ce, Nd, and Yb phosphors with various doping ions concentrations were fabricated by conventional solid-state reaction. Table 1 lists the composition of all the samples. The raw materials of Y_2O_3, Nd_2O_3, CeO_2, Yb_2O_3, and Al_2O_3 with 99.999% purity were weighted according to Table 1, vigorously stirred in alcohol for 24 h, and then dried in air at 80 °C. The obtained samples were ground and transferred into a small alumina crucible covered with an outer crucible filled with sufficient graphite powder. Finally, the samples were calcined in a furnace at 1 500 °C for 24 h in carbon-reducing atmosphere. All of our samples were fabricated under the same condition.

Optical spectroscopy, including fluorescence emission, excitation spectra, fluorescence decay spectra, and lifetime of the samples, were obtained by using a spectrophotometer (FP-6500, JASCO, Japan). All measurements were performed at room temperature.

Figure 1 shows the XRD patterns of YAG-$Ce_{0.05}$, YAG-$Ce_{0.05}Yb_{0.02}$, and YAG-$Ce_{0.05}Yb_{0.02}Nd_{0.05}$. All the pat-

Table 1. Composition of all the Samples

Sample	Composition
A	YAG-$Ce_{0.05}$
B	YAG-$Ce_{0.05}Nd_{0.05}$
C	YAG-$Ce_{0.05}Yb_{0.02}$
D	YAG-$Ce_{0.05}Yb_{0.1}$
E	YAG-$Ce_{0.05}Yb_{0.04}$
F	YAG-$Ce_{0.05}Yb_{0.01}Nd_{0.05}$
G	YAG-$Ce_{0.05}Yb_{0.02}Nd_{0.05}$
H	YAG-$Ce_{0.05}Yb_{0.04}Nd_{0.05}$
I	YAG-$Ce_{0.05}Yb_{0.08}Nd_{0.05}$
J	YAG-$Ce_{0.05}Yb_{0.1}Nd_{0.05}$
K	YAG-$Ce_{0.05}Yb_{0.15}Nd_{0.05}$
L	YAG-$Ce_{0.05}Yb_{0.2}Nd_{0.05}$
M	YAG-$Ce_{0.05}Yb_{0.25}Nd_{0.05}$

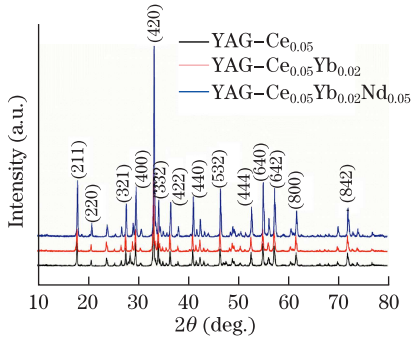

Fig. 1. XRD patterns of YAG-$Ce_{0.05}$, YAG-$Ce_{0.05}Yb_{0.02}$, and YAG-$Ce_{0.05}Yb_{0.02}Nd_{0.05}$ phosphors.

terns are identical to that of cubic YAG (JCPDS 33-0040). Thus, the as-synthesized samples are generally of a single phase.

Emission spectra of YAG-$Ce_{0.05}$, YAG-$Ce_{0.05}Nd_{0.05}$, YAG-$Ce_{0.05}Yb_{0.02}$, and YAG-$Ce_{0.05}Yb_{0.02}Nd_{0.05}$ under 440-nm excitation are plotted in Fig. 2. The emission located at 550 nm is attributed to 5d→4f of Ce^{3+}. Although these samples have similar Ce^{3+}-doping concentration, intensities of 5d→4f of Ce^{3+} emission are different. The intensity of YAG-$Ce_{0.05}$ is the strongest, followed by that of YAG-$Ce_{0.05}Yb_{0.02}$. This result is caused by the energy transfer process of Ce^{3+}, namely, 5d→Yb^{3+}: $^2F_{5/2}$+Yb^{3+}: $^2F_{5/2}$, which weakens the emission of Ce^{3+}[13]. With the addition of Nd^{3+}, the intensity is much weaker, suggesting that higher sensitization efficiency exists between Ce^{3+} and Nd^{3+} than between Ce^{3+} and Yb^{3+} in YAG. Due to the decline of the number of excited-state Ce^{3+}, intensity degradation occurs. Some hollows are observed in the spectrum of YAG-$Ce_{0.05}Nd_{0.05}$ and YAG-$Ce_{0.05}Yb_{0.02}Nd_{0.05}$ between 500 and 650 nm, which are not observed in YAG-$Ce_{0.05}$ and YAG-$Ce_{0.05}Yb_{0.02}$. These hollows are related to the visible absorption of Nd^{3+}[15]. The competitive absorption of Nd^{3+} and Yb^{3+} in YAG-$Ce_{0.05}Yb_{0.02}Nd_{0.05}$ is likely to hinder the energy transfer from Ce^{3+} to Nd^{3+} and Yb^{3+}. Consequently, its emission intensity is a little stronger than that of YAG-$Ce_{0.05}Nd_{0.05}$.

Figure 3 shows the NIR fluorescence spectra of YAG-$Ce_{0.05}Yb_{0.02}$, YAG-$Ce_{0.05}Nd_{0.05}$, and YAG-$Ce_{0.05}Yb_{0.02}Nd_{0.05}$ by 440-nm excitation. The emission peaks at around 900 and 1 060 nm correspond to the Nd^{3+} emission from $^4F_{3/2}$ to $^4I_{9/2}$ and $^4I_{11/2}$, respectively[16]. The observation is a convincing evidence that energy transfer occurs from the relaxed lowest $5d_1$ energy band of Ce^{3+} to the $^2G_{7/2}$ of Nd^{3+}, and then the transferred electrons relax to $^4F_{3/2}$ and decay to the $^4I_{9/2}$ and $^4I_{11/2}$ of Nd^{3+}[14]. According to the emission intensities, the energy transfer is very efficient. However, only one weak emission peak is observed at 1 029 nm in the spectra of YAG-$Ce_{0.05}Yb_{0.02}$, which corresponds to the transfer from $^2F_{5/2}$ to $^2F_{7/2}$ of Yb^{3+}. As seen in Fig. 2, the energy transfer efficiency is much lower than that of YAG-$Ce_{0.05}Nd_{0.05}$. In the spectrum of YAG-$Ce_{0.05}Yb_{0.02}Nd_{0.05}$, the intensity of the emission peak at 1029 nm is about four times stronger than that of YAG-$Ce_{0.05}Yb_{0.02}$. Nd^{3+} has a sensitized role for Yb^{3+}. The possible energy transfer path is Nd^{3+}: $^2G_{9/2}$+ Yb^{3+}: $^2F_{7/2}$ →Nd^{3+}: $^4F_{3/2}$ +Yb^{3+}: $^2F_{5/2}$, Nd^{3+}: $^4F_{3/2}$+ Yb^{3+}: $^2F_{7/2}$ →Nd^{3+}: $^4I_{11/2}$ +Yb^{3+}: $^2F_{5/2}$[17].

The excitation spectra of YAG-$Ce_{0.05}$, YAG-$Ce_{0.05}Yb_{0.1}$, and YAG-$Ce_{0.05}Yb_{0.1}Nd_{0.05}$ are shown in Fig. 4. Based on monitoring results at 570 nm, strong excitation peaks at about 450 and 330 nm are observed in the spectrum of YAG-$Ce_{0.05}$. Similar excitation peaks are also observed in the other two samples (by monitoring at 1 029 nm), except that their intensities are weaker. The similarity in the shape of the excitation peak could be ascribed to the efficient energy transfer from Ce^{3+} to Nd^{3+} and from Ce^{3+} to Yb^{3+}[15,17], which declines in the excited-state numbers and deteriorates the emission of

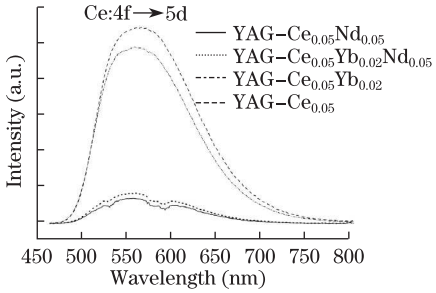

Fig. 2. Emission spectra of YAG-$Ce_{0.05}$, YAG-$Ce_{0.05}Nd_{0.05}$, YAG-$Ce_{0.05}Yb_{0.02}$, and YAG-$Ce_{0.05}Yb_{0.02}Nd_{0.05}$ (λ_{ex} = 440 nm).

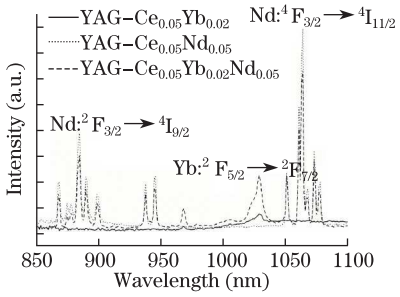

Fig. 3. NIR fluorescence spectra of YAG-$Ce_{0.05}Yb_{0.02}$, YAG-$Ce_{0.05}Nd_{0.05}$, and YAG-$Ce_{0.05}Yb_{0.02}Nd_{0.05}$ by 440-nm excitation.

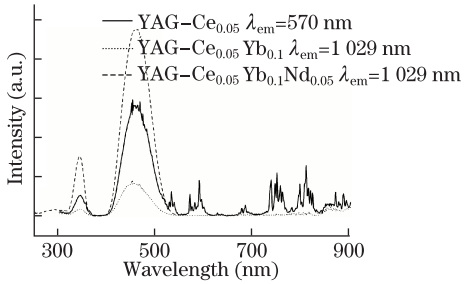

Fig. 4. Excitation spectra of YAG-$Ce_{0.05}$ (λ_{em}= 570 nm), YAG-$Ce_{0.05}Yb_{0.1}$, and YAG-$Ce_{0.05}Yb_{0.1}Nd_{0.05}$ (λ_{em}= 1 029 nm).

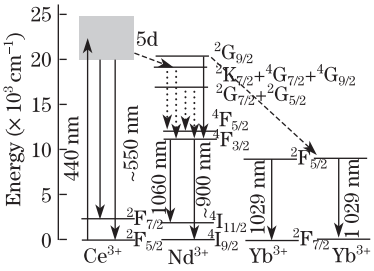

Fig. 5. Simplified energy level diagram with possible energy transfer process in YAG-Ce, Nd, and Yb.

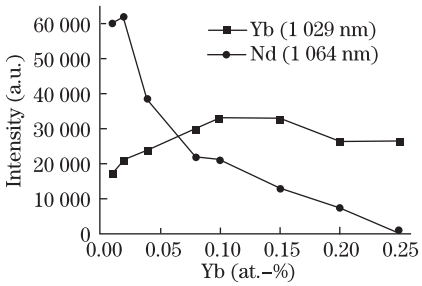

Fig. 6. Fluorescence intensity of Yb^{3+} emission (1029 nm) and Nd^{3+} (1064 nm) as a function of Yb^{3+} doping concentration in YAG-Ce, Nd, and Yb.

Table 2. Calculated Energy Transfer Efficiency η_{ET} as a Function of Yb^{3+}Doping Concentration in YAG-Ce and Yb

Yb^{3+}Concentrations in YAG-Ce and Yb (at.-%)	2	4	10
$\eta_{ET(\%)}$	8.8	15.8	26.6

Ce^{3+}. The intensity at 450 nm of YAG-$Ce_{0.05}Yb_{0.1}Nd_{0.05}$ is much stronger than that of YAG-$Ce_{0.05}Yb_{0.1}$. The energy transfer from Nd^{3+} to Yb^{3+} enhances the excitation spectrum, and the possible path is shown in Fig. 5. Excitation of Nd^{3+} occurs mainly via energy transfer from Ce^{3+}:5d to Nd^{3+}:$^4G_{7/2}$+ $^2G_{7/2}$. After excitation of the 5d state of Ce^{3+}, some electrons can transfer to the ground state of 4f, producing broadband emission. By contrast, other electrons transfer to the excitedlevel of Nd^{3+}. $G_{7/2}$ level corresponds to the excitation band at 530 nm and $^2G_{7/2}$ level corresponds to the excitation band at 592 nm[14]. By further relaxing to a lower-energy level, an emission peak at 890 nm ($^4F_{3/2}$ →$^4I_{9/2}$) can be observed, as shown in Fig. 4. Beyond that, other electrons transfer to the excited state $^2F_{5/2}$ of $Yb^{3+}$and the following emission $^2F_{5/2}$ →$^2F_{7/2}$ occurs due to the energy match between $^2G_{9/2}$ →$^4F_{3/2}$ and $^2F_{5/2}$ →$^2F_{7/2}$.

Table 3. Calculated Energy Transfer Efficiency η_{ET} as a Function of Yb^{3+} Doping Concentrations in YAG-Ce, Nd, and Yb

Concentrations in YAG-Ce, Nd, and Yb (at.-%)	0	1	2	4	10	20	25
η_{ET}(%)	67.6	72.2	70.1	73.3	73.9	79.8	82.8

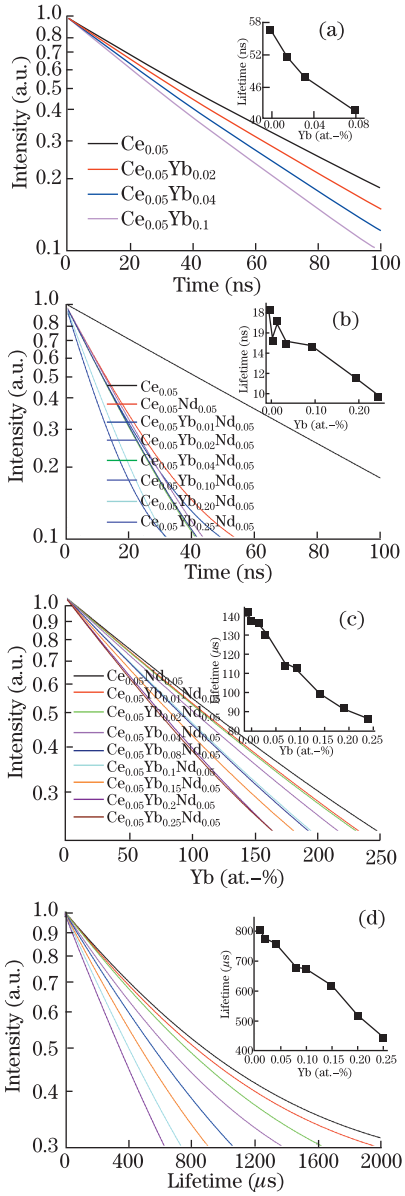

Fig. 7. (a) Colored line is the fitting result of the fluorescence decay curves of Ce^{3+} emission (560 nm) in YAG-Ce and Yb. The inset is the lifetime of Ce^{3+}in YAG-Ce and Yb as the concentration of Yb^{3+} increases. (b), (c), and (d) are the fitting results of the fluorescence decay curves of Ce^{3+} emission (560 nm), Nd^{3+} emission (1 064 nm), and Yb^{3+}emission (1 029 nm), respectively. The insets are their lifetimes with different Yb^{3+} concentrations.

Figure 6 portrays the dependence of Yb^{3+} (1 029 nm) and Nd^{3+} (1 064 nm) emissions on Yb^{3+} doping concentration for YAG-Ce, Nd, and Yb. As Yb^{3+} concentration increases from 1% to 25%, the luminescence of Nd^{3+} monotonically weakens, whereas the intensity of Yb^{3+} first reaches a maximum at 10% Yb^{3+} and then decreases when Yb^{3+} concentration is further increased. This phenomenon indicates the energy transfer from Nd^{3+} to Yb^{3+}. Higher Yb^{3+} concentration promotes the transfer path and accelerates the decay process of Nd^{3+} ($^4F_{3/2} \rightarrow {}^4I_{11/2}$).

The energy transfer from $Ce^{3+}$to Yb^{3+} is further confirmed by the decay lifetime recorded for the Ce^{3+} emission at 560 nm, Nd^{3+} emission at 1064 nm, and Yb^{3+} emission at 1029 nm with different Yb^{3+} concentrations (Fig. 7). The colored lines are the fitting results of the fluorescence decay curves. The decays of Ce^{3+} emission at 560 nm in YAG-$Ce_{0.05}$ can be described by a single exponential. When the samples are co-doped with Yb^{3+}, the faster decays of Ce^{3+} can also be described by a single exponential. The lifetimes of Ce^{3+}emission decrease upon increase of Yb^{3+} concentration. These observations confirm that energy transfer occurs from $Ce^{3+}$to Yb^{3+} in YAG-Ce and Yb, but the efficiency is very low. In Fig. 7(b), the decays are no longer single exponential. The decays in YAG-Ce, Nd, and Yb decrease more rapidly than those in YAG-Ce and Nd. The lifetime of Ce^{3+}in YAG-Ce, Nd, and Yb is remarkably shorter than that in YAG-Ce and Yb. The gradual decline of Nd^{3+}decays with the increase of Yb^{3+} clearly indicates that energy transfer from Nd^{3+} to Yb^{3+} occurs, which is consistent with the intensity of Nd^{3+}emission (Fig. 6). As observed in Figs. 7(c) and (d), the decreased lifetime of Nd^{3+} emission at 1 064 nm in YAG-Ce, Nd, and Yb is the result of the energy transfer ($Nd^{3+} \rightarrow Yb^{3+}$), whereas the reduction of the lifetime of Yb^{3+} emission at 1 029 nm is attributed to the reduced concentration. The lifetime decrease of Nd^{3+} further verifies the presence of energy transfer ($Nd^{3+} \rightarrow Yb^{3+}$). The mechanism of concentration quenching can be described as follows: resonant excitation energy migration between Yb^{3+} occurs, and this process makes part of the energy transferred to quenching centers evolve into impurities or defects. If the concentration of Yb^{3+} increases, this energy migration will become faster[18].

We estimated the Ce-Yb energy transfer efficiency η_{ET} by using the following equation[13]:

$$\eta_{ET} = 1 - \tau_x/\tau_0,$$

where τ_x and τ_0 represent the decay lifetimes of Ce^{3+} at 560 nm of samples with Yb^{3+} doping concentration of x and x= 0, respectively. Tables 2 and 3 list the η_{ET} of YAG-Ce and Yb and YAG-Ce, Nd, and Yb, which exhibit a monotonous increase with the doping concentration of Yb^{3+}. The corresponding η_{ET} of YAG-Ce, Nd, and Yb is larger than that of YAG-Ce and Yb when they have the same Yb^{3+}doping concentration. The η_{ET} of YAG-Ce and Nd is lower than that in triple-doped systems. The conclusion that Nd^{3+} improves the energy transfer from $Ce^{3+}$to Yb^{3+}can be drawn based from these observations. With a high efficiency of 82.8%, YAG-Ce, Nd, and Yb phosphors may find potential application in improving the efficiency of silicon-based solar cells.

In conclusion, the energy transfer from Ce^{3+} to Yb^{3+}, from Ce^{3+} to Nd^{3+}, and from Nd^{3+} to Yb^{3+}, as well as the sensitized luminescence of Yb^{3+}in YAG-Ce, Nd, and Yb phosphors, are investigated by excitation spectra, emission spectra, and fluorescence decay spectra. Results indicate that Nd^{3+} can function as a sensitizer ion for Yb^{3+}, improving the energy transfer from Ce^{3+} to Yb^{3+}. The possible path is Ce^{3+}: 5d→Nd^{3+}: $^2G_{9/2}$ →Yb^{3+}: $^2F_{5/2}$. The energy transfer efficiency of Ce^{3+} reaches as high as 82.8% in YAG-Ce, Nd, and Yb, which is much higher than that in YAG-Ce and Nd and YAG-Ce and Yb. The intense NIR emission, which is in the spectral response wavelength of the solar cells, can be easily excited by visible light (440 nm) in the triple-doped phosphor. Therefore, YAG-Ce, Nd, and Yb with high energy transfer efficiency may be a promising candidate for phosphor downconversion to optimize Si solar cell performance.

This work was supported by the National Natural Science Foundation of China (No. 61078054) and the Science and Technology Commission of Shanghai Municipality (No. 11DZ1140301).

References

1. T. Trupke, M. A. Green, and P. Wurfel, J. Appl. Phys. **92,** 1668 (2002).
2. M. Zhang, Y. Ren, D. C. Cheng, and M. Lu, Chin. Opt. Lett. **10,** 063101 (2012).
3. J. A. Pardo, J. L. Pena, R. L. Merino, R. Cases, A. Larrea, and V. M. Orera, J. Non-Cryst. Solids **298,** 23 (2002).
4. W. Shockley and H. J. Queisser, J. Appl. Phys. **32,** 510 (1961).
5. Q. Zhang and X. Huang, Prog. Mater. Sci. **55,** 353 (2010).
6. S. Ye, N. Jiang, F. He, X. Liu, B. Zhu, Y. Teng, and J. R. Qiu, Opt. Express **18,** 639 (2010).
7. W. StrJk, A. Bednarkiewicz, and P. J. Deren, J. Lumin. **92,** 229 (2001).
8. Q. Zhang, G. Yang, and Z. Jiang, Appl. Phys. Lett. **91,** 051903 (2007).
9. X. Liu, Y. Qiao, G. Dong, S. Ye, B. Zhu, G. Lakshminarayana, D. Chen, and J. Qiu, Opt. Lett. **33,** 2858 (2008).
10. H. Zhang, Y. Wang, and L. Han, J. Appl. Phys. **109,** 053109 (2011).
11. H. Lin, S. Zhou, H. Teng, Y. Li, W. Li, X. Hou, and T. Jia, J. Appl. Phys. **107,** 043107 (2010).
12. J. Zhong, C. Liu, H. Liang, Q. Su, J. Zhou, and J. Wang, Opt. Mater. **34,** 152 (2011).
13. X. Liu, Y. Teng, Y. Zhuang, J. Xie, Y. Qiao, G. Dong, D. Chen, and J. Qiu, Opt. Lett. **34,** 3565 (2009).
14. J. Meng, J. Li, P. Zhao, and K. W. Cheah, Appl. Phys. Lett. **93,** 221908 (2008).
15. Y. Li, S. Zhou, H. Lin, X. Hou, and W. Li, Opt. Mater. **32,** 1223 (2010).
16. O. G. Okhotnikov and J. R. Salcedo, Appl. Phys. Lett. **64,** 2619 (1994).
17. D. Chen, Y. Yu, H. Lin, P. Huang, Z. Shan, and Y. Wang, Opt. Lett. **35,** 220 (2010).
18. K. Petermann, D. Fagundes-Peters, J. Johannsen, M. Mond, V. Peters, J. J. Romero, S. Kutovoi, J. Speiser, and A. Giesen, J. Cryst. Growth **275,** 135 (2005).